*Proceedings of the 11th International Conference on Fluid Flow, Heat and Mass Transfer (FFHMT 2024)*
*Chestnut Conference Centre - University of Toronto, Toronto, Canada – June 16-18, 2024*
*Paper No. 093*
*DOI: 10.11159/ffhmt24.093*

# Self-similarity in Turbulent Free Jets: A Study of Triangular and Round Jets

**Mohammad Azad**
St. Francis Xavier University
Antigonish, Nova Scotia, Canada
mazad@stfx.ca

***Abstract*** - This paper presents experimental findings on a turbulent free jet emanating from an isosceles triangular orifice with a 70° apex angle. Comparative measurements were conducted in a round jet issuing from a sharp-edged orifice and a jet issuing from an isosceles triangular orifice with an apex angle of 10°. The Reynolds number, based on the exit centreline velocity and the equivalent diameter of the triangular orifices, or the diameter of the round orifice, was $(1.56 \pm 0.12) \times 10^5$. Data were acquired using a DANTEC P51 x-wire hot wire probe calibrated with a Pitot-Static tube. Profiles of mean streamwise velocity, streamwise and spanwise turbulence intensities, and spanwise Reynolds primary shear stresses along the spanwise direction were obtained. Findings indicate that the mean streamwise velocity profiles of the 70° triangular jet achieve self-similarity 10 diameters downstream. The spanwise turbulence intensity and Reynolds primary shear stress achieve self-similarity 15 diameters downstream of the jet exit plane. Additionally, the results suggest that the jets retain their initial conditions within 25 diameters downstream, as profiles other than mean streamwise velocity profiles of the three jets do not collapse onto the same curve.

***Keywords*****:** Turbulent jet, Triangular, Orifice, Self-similarity

## 1. Introduction

The self-similarity of turbulent jets is a subject of extensive research due to its significance in unravelling the complexities inherent in turbulent flows. Numerous studies have highlighted that turbulent free jets tend to lose their distinctive characteristics far downstream from their origin, exhibiting similar behaviours [1 – 4]. Some studies suggest that this region is not entirely independent of initial conditions [5 – 8]. Some researchers have emphasized that the collapse of mean velocity profiles to a single curve, when they are plotted using a velocity scale and a length scale, doesn't necessarily imply independence from initial conditions but rather indicates a streamwise dependence on normalizing scales [9]. A group of researchers addressed this discrepancy by defining strong self-similarity, which they called self-preserving, and weak self-similarity [10]. In the case of self-preserving flow, all the velocity profiles and other quantities can be normalized using a single velocity and a length scale. On the other hand, a weaker self-similarity exists when each dependent variable is allowed to have its own scale.

Among different initial conditions, jets can have differences in exit velocity profiles, nozzle shape, Reynolds number, aspect ratio of noncircular nozzles, and nozzle profile (contoured, orifice, pipe etc.). Experiments conducted comparing jets from different nozzles demonstrated that a jet from a round smooth contraction nozzle reaches self-similarity faster than one from a round pipe due to differences in their exit velocity profiles [11]. Additionally, others found that Reynolds numbers affect the self-similarity of jets, with higher Reynolds numbers leading to self-similar velocity profiles closer to the nozzle exit [12]. They found self-similarity of streamwise and spanwise turbulence intensities also depends on Reynolds number. A study on plane jets further demonstrated that the velocity profiles become self-similar at shorter downstream distances as the Reynolds number increases [13]. However, studies also suggest that while mean statistics remain largely unaffected by the initial conditions, turbulence statistics are influenced [14].

In a study of a round jet, it was observed that both mean streamwise velocity profiles and higher-order turbulence statistics became self-similar in the fully developed region, albeit at varying downstream distances [15]. In this study on a round jet with a Reynolds number of $10^5$, the mean streamwise velocity profiles became self-similar 20 diameters downstream of the jet exit plane and the streamwise turbulence intensity became self-similar 40 diameters downstream, while the spanwise and lateral turbulence intensities became self-similar 70 diameters downstream. However, another study found

that the mean streamwise velocity profiles of a round jet with a Reynolds number of $10^5$ became self-similar 30 diameters downstream [16]. It was also observed that the mean streamwise velocity field of a jet issuing from a round orifice achieved self-similarity at 8 diameters downstream, but the turbulence field did not reach self-similarity within 16 diameters downstream, which was the streamwise limit for this study [17]. Another study extended this understanding, showing that the mean streamwise velocity profiles for jets from different nozzle geometries achieve self-similarity at similar downstream distances [18]. This study used round, cross, and rectangular jets. The self-similar velocity profiles followed the Gaussian distribution $U/U_{cl} = e^{-(Y/Y_{1/2})^2 \cdot ln2}$ , where $U$ is the local velocity, $U_{cl}$ is the velocity on the jet centreline, and $Y_{1/2}$ is the jet half-velocity width in the spanwise direction.

This paper aims to explore the self-similarity of a jet issuing from an isosceles triangular orifice with an apex angle of 70°. In the far field, self-similarity will be explored for jets issuing from a sharp-edged round orifice and an isosceles triangular orifice with an apex angle of 10°. The scope of this study is restricted to streamwise and spanwise first and second-order quantities.

## 2. Experimental Setup

A comprehensive description of the flow facility and its equipment has been provided elsewhere [19]. In summary, the setup included a blowdown flow system consisting of a centrifugal fan, diffuser, settling chamber, and contraction. The centrifugal fan, mounted on anti-vibration neoprene pads, drew air and delivered it through a flexible duct to the orifices via the diffuser, settling chamber, and contraction. The diffuser, equipped with honeycomb and mesh-wire screens, had a divergence angle of 9°. The settling chamber housed seven mesh-wire screens with 69% porosity. The contraction featured a circular upstream end and a square downstream end capped by the orifices, with a contraction ratio of 283. A schematic of the triangular orifice with an apex angle of 70°, adapted from Azad [20], is shown in Fig. 1. The streamwise ($X$), spanwise ($Y$), and lateral (Z) coordinates are depicted in this figure.

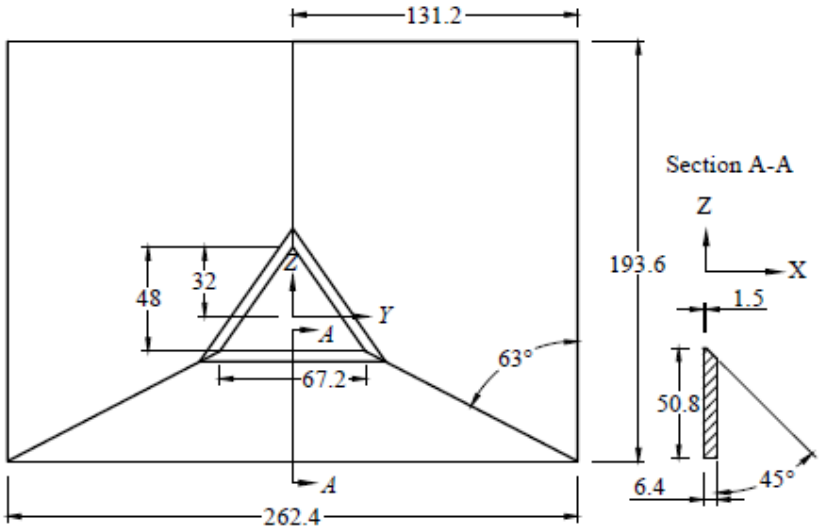


Fig. 1: The schematic of the isosceles triangular orifice with an apex angle of 70° [20]. All dimensions are in mm.

Additionally, a three-dimensional traversing system, also supported by anti-vibration neoprene pads, facilitated the movement of the measuring probes within the flow field. This system offered positioning accuracy of 0.3 mm in the streamwise direction and 0.01 mm in the spanwise and lateral directions.

The measurement tools included a Pitot-Static tube with an ellipsoidal head and four circumferentially placed static pressure holes, along with a DANTEC P51 x-array hot-wire probe. The hot-wire probe underwent in-situ online calibration for velocity and yaw following Bradshaw's method [21]. Velocity calibration was conducted against known values obtained

by the Pitot-Static tube within a velocity range of 8 m/s to 65 m/s. Yaw calibration involved comparing hot-wire voltages within an angular range of -35° to 35° in 5° increments. Temperature monitoring was achieved using a thermocouple near the hot-wire probe and Pitot-Static tube, with temperature drift corrections applied in the data reduction software as per Bearman's method [22]. Signals from the hot-wire probe and thermocouple were linearized and digitized following Quinn's description [23].

## 3. Initial Conditions

Figure 2 illustrates the mean streamwise velocity profile of the 70° triangular jet at $X/D_e$ = 0.14. Here, $U$ is the mean streamwise velocity anywhere along $Y$ axis, $U_{cl}$ is the mean streamwise velocity at the centre, $Y_{1/2}$ is the distance along $Y$ axis from the centre where $U = 1/2U_{cl}$, $X$ is the streamwise distance, and $D_e$ is the equivalent diameter of the triangular orifice. The equivalent diameter of the triangular orifice was calculated as $D_e = \sqrt{4A/\pi}$, where $A$ is the orifice exit area. The profile displays uniformity in the central region while exhibiting distinct off-centre peaks near the jet edges, a common feature not only in triangular jets but also in other orifice jets.

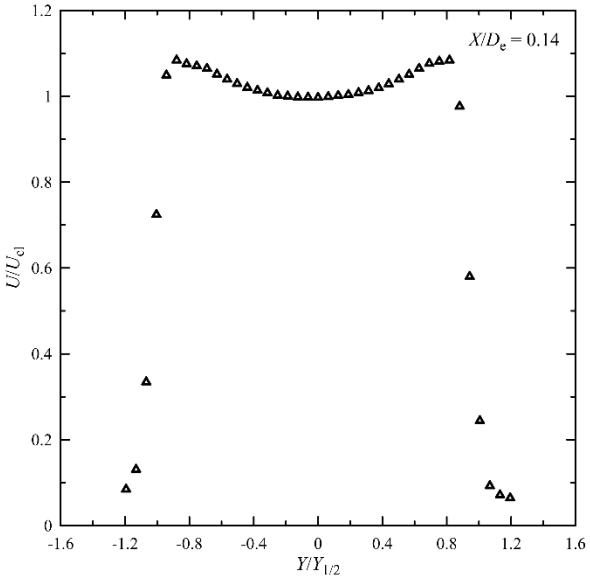


Fig. 2: Mean streamwise velocity profile close to the orifice exit plane.

The $Y$-profiles of streamwise ($\sqrt{\overline{u'^2}}/U_{cl}$) and spanwise ($\sqrt{\overline{v'^2}}/U_{cl}$) turbulence intensities at $X/D_e$ = 0.14, the same streamwise location where the $U/U_{cl}$ profile has been presented, are depicted in Figs. 3(a) and 3(b), respectively. In the central region where the $U/U_{cl}$ profile is nearly uniform, the $\sqrt{\overline{u'^2}}/U_{cl}$ profile appears flat. The value of streamwise turbulence intensity is approximately 0.4% at the center and peaks at around 7% in the shear layers. The $\sqrt{\overline{v'^2}}/U_{cl}$ profile mirrors the $\sqrt{\overline{u'^2}}/U_{cl}$ profile but with lower values as expected. The spanwise turbulence intensity is approximately 0.1% in the central region and increases to 6% in the shear layers.

## 4. Results and Discussion

The uncertainties in different measured and derived quantities were calculated at $X/D_e$ = 5 using the multiple-sample theorem method given by Tavoularis [24]. The uncertainties in mean streamwise velocity ($U$), mean square of streamwise fluctuation ($\overline{u'^2}$), mean square of spanwise fluctuation ($\overline{v'^2}$), and spanwise Renolds primary shear stress ($\overline{u'v'}$) at 95% confidence interval were ±0.71%, ±4.21%, ±7.2%, and ±11.5%, respectively.

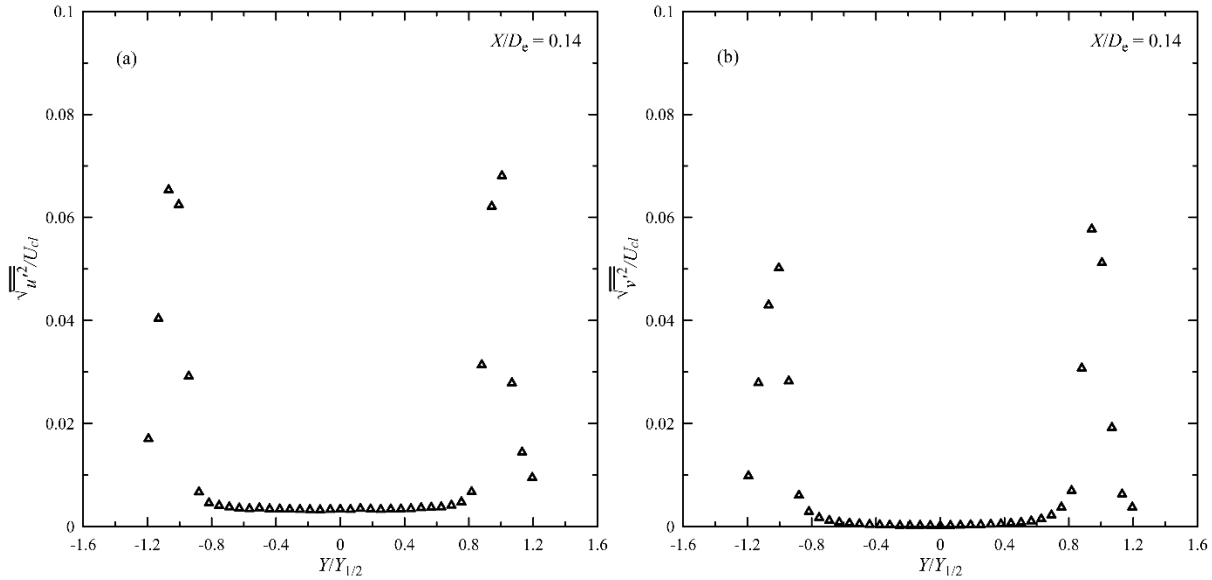

Fig. 3: Turbulence intensity profiles close to the orifice exit plane: (a) streamwise and (b) spanwise.

### 4.1. Near Field Mean Velocity and Turbulence Profiles

The near field spanwise profiles of mean streamwise velocity, streamwise turbulence intensity, spanwise turbulence intensity, and spanwise Reynolds primary shear stress are presented in Fig. 4. The mean streamwise velocity profile at $X/D_e$ = 0.25 exhibits off-centre peaks, as seen in the profile at $X/D_e$ = 0.14. As the jet evolves downstream, the off-centre peaks flatten, and the velocity profile becomes flat at $X/D_e$ = 0.5. At $X/D_e$ = 7, the velocity profile transforms into a 'bell shape' with wide tails. The velocity profiles are not self-similar in this near-field region.

Both streamwise and spanwise turbulence intensity profiles are characterized by off-centre peaks and low turbulence intensities in the central region. These off-centre peaks in the near flow field are expected as turbulence intensities are generated through local shear in the mean streamwise velocity away from the jet centre. As the jet evolves downstream, these shear layers move closer to the jet centreline, and so do the off-centre peaks in the turbulence intensity profiles. Streamwise turbulence intensities are generated from the shear in the mean flow, and spanwise turbulence intensities are generated from streamwise turbulence intensities via fluctuations in jet pressure. Hence these profiles are similar, but streamwise turbulence intensities are stronger than spanwise turbulence intensities.

Spanwise Reynolds primary shear stress is zero at the centre of the jet and exhibits off-centre peaks when turbulence intensities have their peaks. As the jet evolves, the peaks in the Reynolds shear stress profiles move toward the jet centreline. As evident from Fig. 4, none of the profiles reaches self-similarity in this near flow field.

### 4.2. Far Field Mean Velocity and Turbulence Profiles

The mean streamwise velocity, streamwise turbulence intensity, spanwise turbulence intensity, and spanwise Reynolds primary shear stress profiles in the far flow field are presented in Fig. 5. The mean streamwise velocity profiles, normalized by the local centerline velocity and the local half-velocity width, collapse into a single curve represented by the Gaussian distribution:

$$U/U_{cl} = e^{-\left(Y/Y_{1/2}\right)^2 \cdot ln2} \tag{1}$$

As mentioned by others [18], based on the collapse of the mean streamwise velocity profiles into the Gaussian distribution, it can be said that the mean streamwise velocity profiles reach self-similarity 10 diameters downstream of the jet exit plane.

It should be noted that velocity profiles in the outer region of the jet do not quite align with the Gaussian distribution as they do in the inner region of the jet. It is known that the uncertainty in the results obtained by a hot wire anemometer close to the boundary of the jet is higher due to flow reversal. Figure 5 shows that the spanwise turbulence intensity and Reynolds primary shear stress achieve self-similarity 15 diameters downstream of the jet exit plane.

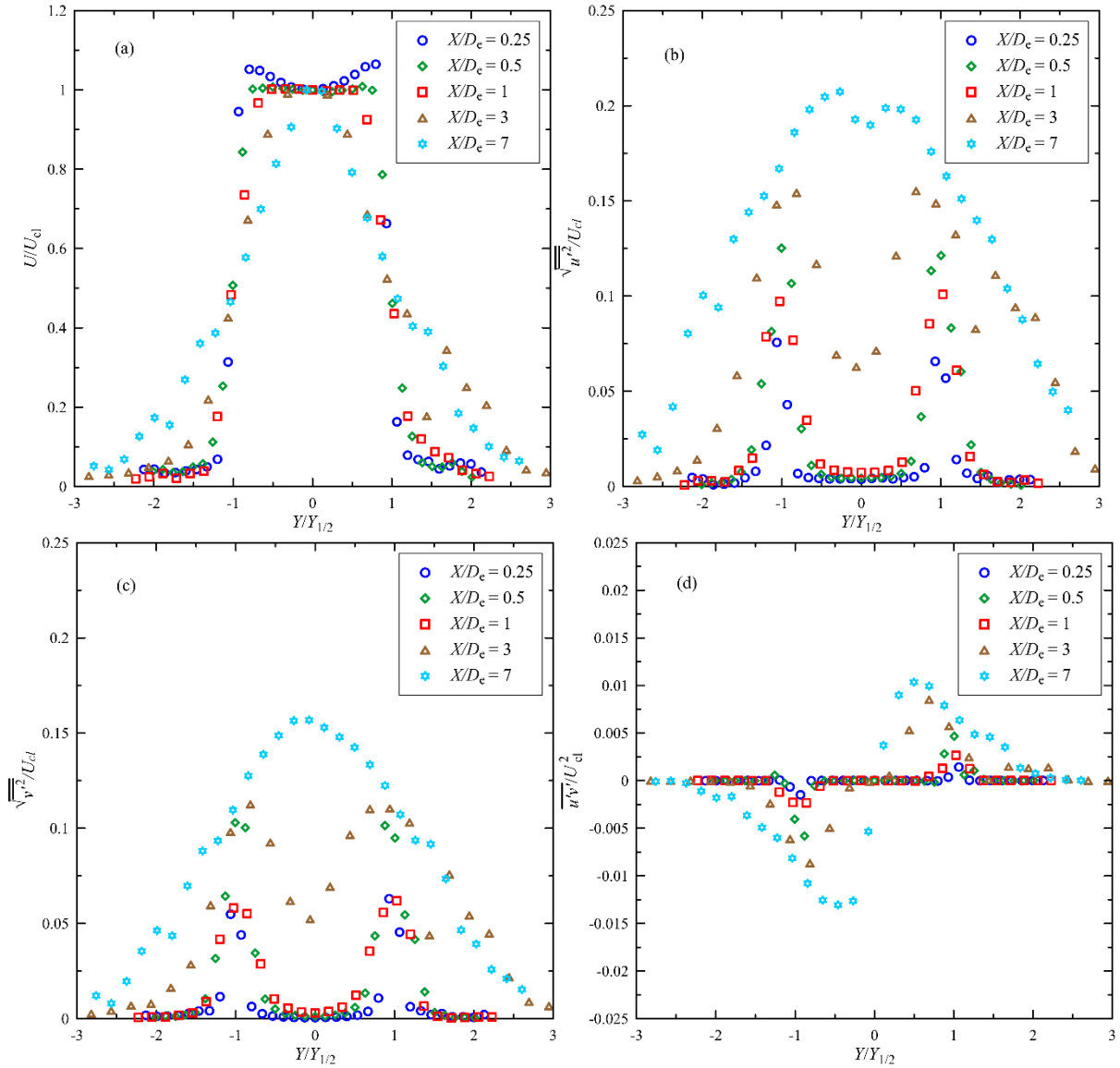


Fig. 4: Near field profiles of the 70° triangular jet: (a) mean streamwise velocity, (b) streamwise turbulence intensity, (c) spanwise turbulence intensity, and (d) Reynolds primary spanwise shear stress.

### 4.3. Far Field Profiles of Other Jets

The mean streamwise velocity, streamwise turbulence intensity, spanwise turbulence intensity, and spanwise Reynolds primary shear stress profiles for the jets issuing from 10° and 70° isosceles triangular orifices and a sharp-edged round orifice are presented for *X/De* = 25 in Fig. 6. The mean streamwise velocity profiles of all the jets collapse into the Gaussian distribution curve (Eq. 1), indicating self-similarity in those profiles. This indicates that the jets have forgotten their initial conditions, at least for the mean streamwise velocity profiles. The streamwise turbulence intensity, spanwise turbulence

intensity, and spanwise Reynolds primary shear stress profiles of these jets do not collapse onto a single curve, indicating that the jets are not self-preserving, at least in the range tested in the present study. This finding contradicts the findings of Afriyie [18], although the studied jets are different.

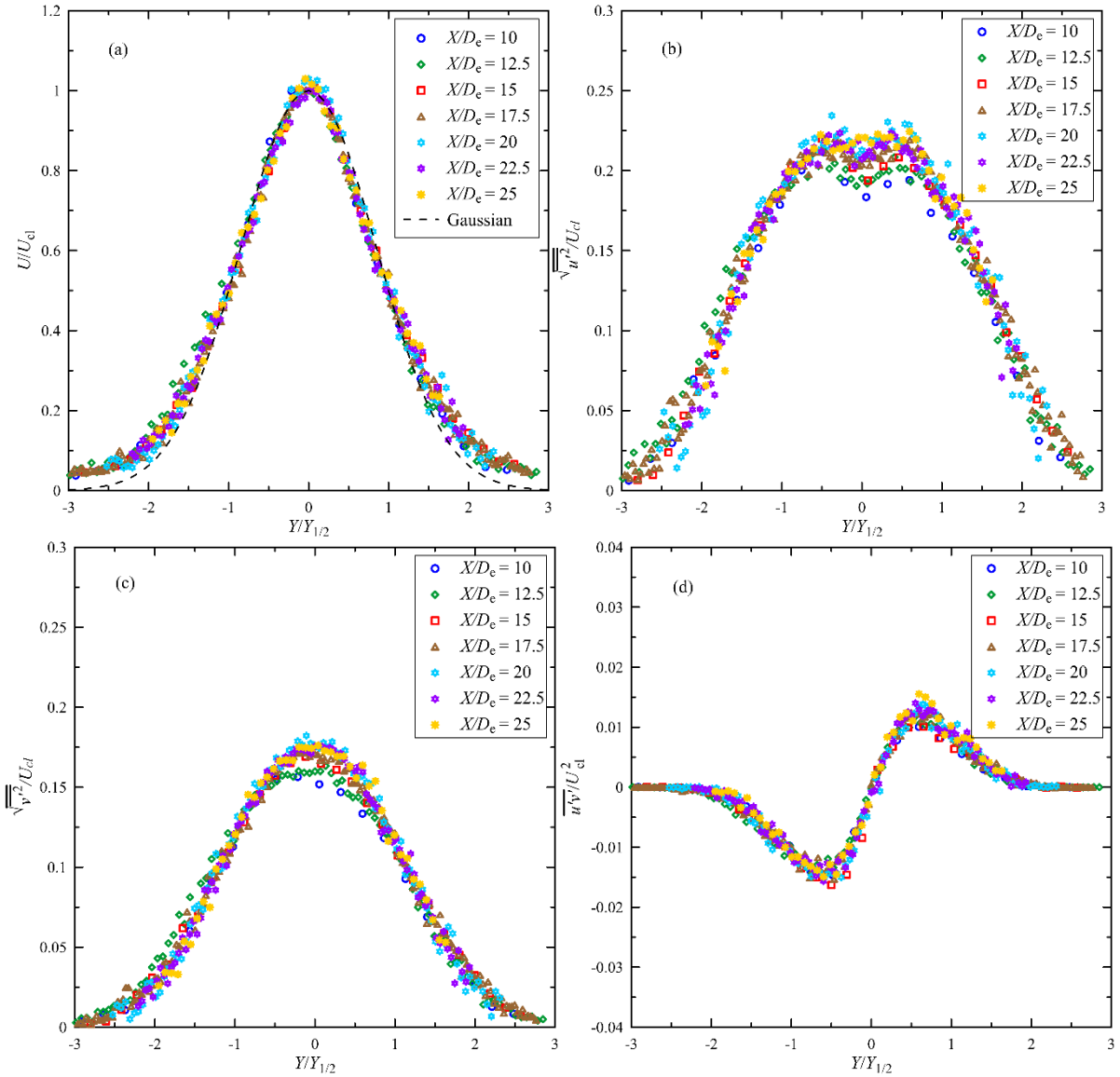


Fig. 5: Far-field profiles of the 70° triangular jet: (a) mean streamwise velocity, (b) streamwise turbulence intensity, (c) spanwise turbulence intensity, and (d) Reynolds primary spanwise shear stress.

## 5. Conclusion

A turbulent jet issuing from an isosceles triangular orifice with an apex angle of 70° has been thoroughly studied for self-similarity. The mean velocity field of this jet achieves self-similarity 10 diameters downstream from the jet exit plane. The spanwise turbulence intensity, and spanwise Reynolds primary shear stress reach self-similarity 15 diameters downstream from the jet exit plane. The trace of jet initial conditions cannot be observed in the mean flow field of the 10° and 70° triangular and round jets at 25 diameters downstream from the jet exit plane. However, the effects of initial conditions

(geometry of the orifice) are present in the streamwise turbulence intensity, spanwise turbulence intensity, and spanwise Reynolds primary shear stress profiles of these jets even 25 diameters downstream from the jet exit plane.

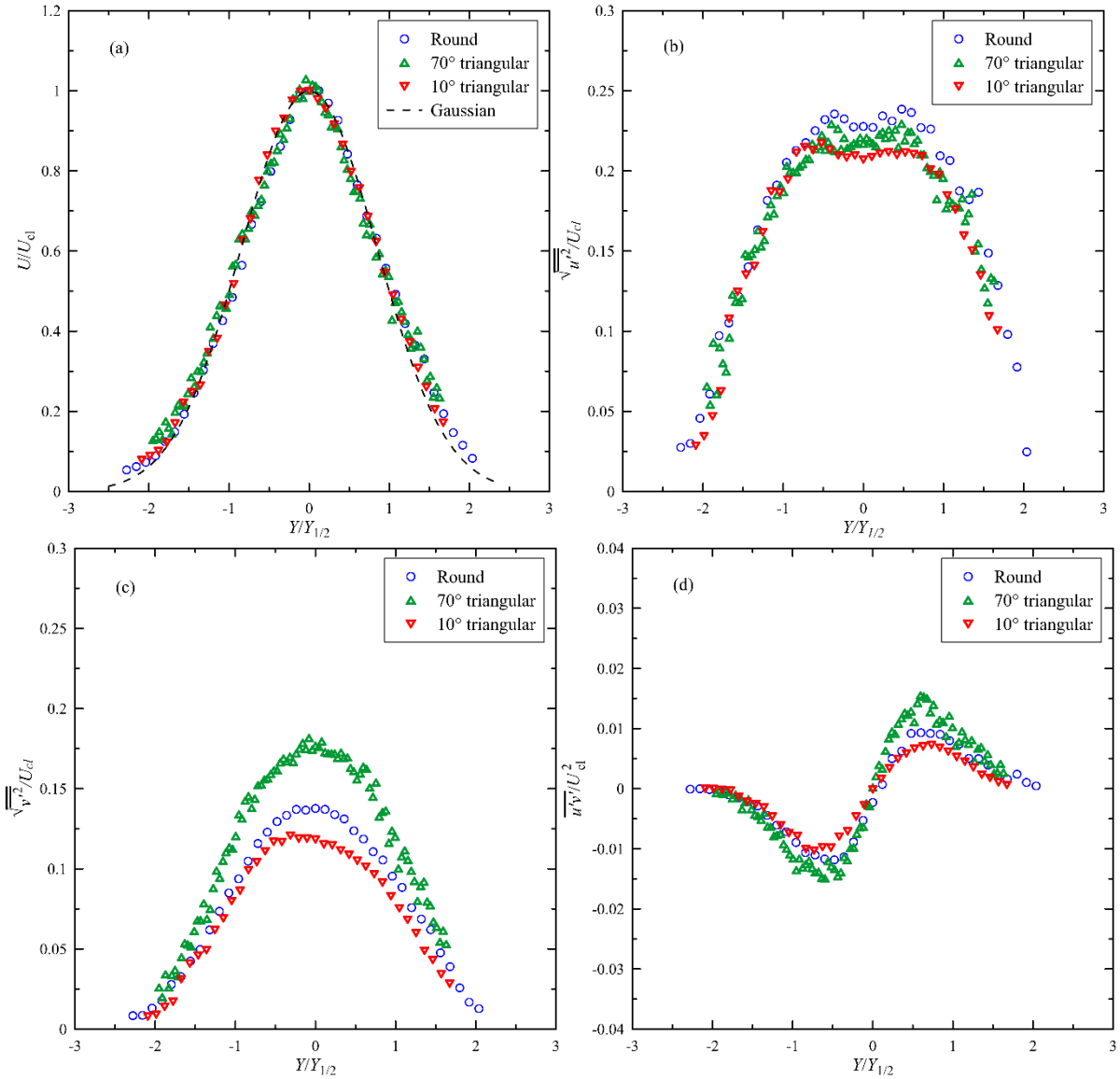


Fig. 6: Far-field profiles of different jets: (a) mean streamwise velocity, (b) streamwise turbulence intensity, (c) spanwise turbulence intensity, and (d) Reynolds primary spanwise shear stress.

## References


[1] D. R. Dowling and P. E. Dimotakis, "Similarity of the concentration field of gas-phase turbulent jets," J. Fluid Mech., vol. 218, pp. 109–141, 1990.

[2] W. M. Pitts, "Reynolds number effects on the centreline mixing behavior of axisymetric turbulent jets," Exp. Fluids, vol. 11, pp. 135-144, 1991.

[3] C. D. D. Richards and W. M. Pitts, "Global density effects on the self-preservation behaviour of turbulent free jets," J. Fluid Mech., vol. 254, pp. 417-435, 1993.

[4] R. A. Antonia and Q. Zhao, “Effect of initial conditions on a circular jet,” Exp. Fluids, vol. 31, pp. 319–323, 2001.
[5] W. K. George, “The self-preservation of turbulent flows and its relation to initial conditions and coherent structures,” Advances in Turbulence, Hemisphere, New York, 1989, pp.39-73.
[6] J. Mi, D. S. Nobes, and G. J. Nathan, “Influence of jet exit conditions on the passive scalar field of an axisymmetric free jet,” J. Fluid Mech., vol. 432, pp. 91-125, 2001.
[7] B. J. Boersma, G. Brethouwer, and F. T. M. Nieuwstadt, “A numerical investigation on the effect of inflow conditions on the self-similar region of a round jet,” Phys. Fluids, vol. 10, no. 4, pp. 899–909, 1998.
[8] E. Ferdman, M. V. Otugen, and S. Kim, “Effect of initial velocity profile on the development of the round jet,” J. Propul. Power, vol. 16, no. 4, pp. 676-686, 2000.
[9] W. K. George and L. Davidson, “Role of Initial Conditions in Establishing Asymptotic Flow Behavior,” AIAA J., vol. 42, no. 3, pp. 438- 446, 2004.
[10] D. Sciamarella, F. Silva, and G. Artana, “Similarity analysis of a glottal-like jet,” Exp. Fluids, vol. 53, pp. 765–776, 2012.
[11] G. Xu, and R. A. Antonia, “Effect of different initial conditions on a turbulent round free jet,” Exp. Fluids, vol. 33, pp. 677–683, 2002.
[12] M. Xu, A. Pollard, J. Mi, F. Secretain, and H. Sadeghi, “Effects of Reynolds number on some properties of a turbulent jet from a long square pipe,” Phys. Fluids, vol. 25, no. 3, 035102, 2013.
[13] R. C. Deo, J. Mi, and G. J. Nathan, “The influence of Reynolds number on a plane jet,” Phys. Fluids, vol. 20, no. 7, 075108, 2008.
[14] M. Uddin and A. Pollard, “Self-similarity of coflowing jets, the virtual origin,” Phys. Fluids, vol. 19, no. 6, pp. 68103/1–68103/4, 2007.
[15] I. Wygnanski and H. Fiedler, “Some measurements in the self-preserving jet,” J. Fluid Mech., vol. 38, pp. 577–612, 1969.
[16] H. J. Hussein, S. P. Capp, and W. K. George, “Velocity measurements in a high-Reynolds number, momentum-conserving, axisymmetric, turbulent jet,” J. Fluid Mech., vol. 258, pp. 31–75, 1994.
[17] J. Mi, P. Kalt, G. J. Nathan, and C. Y. Wong, “PIV measurements of a turbulent jet issuing from round sharp-edged plate,” Exp. Fluids, vol. 42, no. 4, pp. 625–637, 2007.
[18] Y. Y. Afriyie, “Effect of Nozzle Geometry on Mixing Characteristics of Turbulent Free Orifice Jets,” M.Sc. Thesis, Dept. Mech. Eng., University of Manitoba, Manitoba, 2017.
[19] M. Azad, W. R. Quinn, and D. Groulx, “Mixing in turbulent free jets issuing from isosceles triangular orifices with different apex angles,” Exp. Thermal and Fluid Sci., vol. 39, pp. 237-251, 2012.
[20] M. Azad, “Effects of Apex Angle Variation on Flow Development in Jets Issuing from Different Isosceles Triangular Orifices,” M.A.Sc. Thesis, Dept. Mech. Eng., Dalhousie University, Halifax, 2011.
[21] P. Bradshaw, “An Introduction to Turbulence and its Measurement,” Oxford, Pergamon Press, 1975.
[22] P. W. Bearman, “Corrections for the Effect of Ambient Temperature Drift on Hot-wire Measurements in Incompressible Flow,” DISA Info, vol. 11, no. 11, pp. 25-30, 1971.
[23] W. R. Quinn, “Upstream Nozzle Shaping Effects on Near Field Flow in Round Turbulent Free Jets,” European J. Mech. B/Fluids, vol. 25, no. 3, pp. 279–301, 2006.
[24] S. Tavoularis, “Measurements in Fluid Mechanics” Cambridge, Cambridge University Press, 2005.